

SHAPES OF STELLAR SYSTEMS AND DARK HALOS FROM SIMULATIONS OF GALAXY MAJOR MERGERS

GREGORY S. NOVAK,¹ THOMAS J. COX,² JOEL R. PRIMACK,³ PATRIK JONSSON³, AVISHAI DEKEL⁴

Draft version July 7, 2018

ABSTRACT

Using a sample of 89 snapshots from 58 hydrodynamic binary galaxy major merger simulations, we find that stellar remnants are mostly oblate while dark matter halos are mostly prolate or triaxial. The stellar minor axis and the halo major axis are almost always nearly perpendicular. This can be understood by considering the influence of angular momentum and dissipation during the merger. If binary mergers of spiral galaxies are responsible for the formation of elliptical galaxies or some subpopulation thereof, these galaxies can be expected to be oblate and inhabit their halos with the predicted shapes and orientations. These predictions are relevant to observational studies of weak gravitational lensing, where one must stack many optically aligned galaxies in order to determine the shape of the resulting stacked mass distribution. The simple relationship between the dark and luminous matter presented here can be used to guide the stacking of galaxies to minimize the information lost.

Subject headings: galaxies: formation — galaxies: interactions — galaxies: kinematics and dynamics — galaxies: structure

1. INTRODUCTION

The shapes and mass profiles of dark matter halos from cosmological N -body simulations have long been studied (Dubinski & Carlberg 1991; Navarro et al. 1996; Allgood et al. 2006, and references therein). Cosmological simulations still lack sufficient resolution to track the shape and orientation of galaxies within their dark matter halos. There is no reason to believe that the shapes of galaxies and dark matter halos should be similar. It has only recently become feasible to perform large suites of high-resolution binary galaxy merger simulations (Naab & Burkert 2003; Cox 2004; Cox et al. 2005; Robertson et al. 2006), and we here use such simulations in order to study the shapes of the resulting galaxies and their host halos statistically.

Observationally, the intrinsic shapes of elliptical galaxies have remained elusive. It has long been known that there seem to be at least two classes of elliptical galaxies: massive, anisotropic galaxies and lower mass, oblate rotators (Bender et al. 1988, 1992). However, allowing the possibility of triaxiality leads to degeneracies in deprojection (Franx et al. 1991). Alam & Ryden (2002) and Vincent & Ryden (2005) have used Sloan Digital Sky Survey (SDSS) data to conclude that not all elliptical galaxies can be oblate.

The relative orientations of galaxies and their dark halos is relevant to studies of weak gravitational lensing. Observers stack many images of galaxies in order to use the average deformation of the shapes of background galaxies to infer properties of the foreground mass dis-

tribution. It is important to stack galaxies coherently in order to build up a detectable signal. The model presented here represents a physically well-motivated *Ansatz* to help interpret the results of weak lensing observations. Section 2 gives a description of the galaxy merger simulations and our method of determining the shape of merger remnants, §3 gives our results, and §4 summarizes our conclusions.

2. METHODS

We analyze the shapes of 89 snapshots from 58 of these simulations. We study two samples of simulations. One is the “G” series, which consists of major and minor mergers with progenitor spiral galaxies typical of the nearby universe and spanning a factor of 40 in baryonic mass and 20 total mass. In order to reduce the dependence on the progenitor galaxy model, here we only consider major mergers with mass ratios of 1:1 (G3-G3, G2-G2, G1-G1, and G0-G0) and roughly 3:1 (G3-G2, G2-G1, and G1-G0). We also analyze the “Sbc” series of merger simulations, which are 1:1 major mergers of massive, gas-rich spirals using a variety of different orbits and orientations.

To calculate the shape of a merger remnant, we iteratively diagonalize a moment of inertia tensor using an ellipsoidal window (Dubinski & Carlberg 1991):

$$M_{ij} = \sum_k m_k r_{i,k} r_{j,k} \quad (1)$$

where $r_{i,k}$ is the position vector, i, j refer to coordinates, and k refers to particle number. The triaxial radius is given by Franx et al. (1991):

$$\zeta = \sqrt{x^2/a^2 + y^2/b^2 + z^2/c^2} \quad (2)$$

where a , b , and c are the major, intermediate, and minor axis lengths, respectively. The sum over k includes all particles for which r lies within the ellipsoid $\zeta = 1$. The iteration is started with a spherical window ($a = b = c =$ baryonic half-mass radius), and after each iteration a, b , and c are scaled so that half of the baryonic mass

arXiv:astro-ph/0604121v2 22 Jul 2006

¹ UCO/Lick Observatories, University of California, 1156 High Street, Santa Cruz, CA 95064; novak@ucolick.org

² Harvard-Smithsonian Center for Astrophysics, 60 Garden Street, Cambridge, MA 02138; tcox@cfa.harvard.edu

³ Department of Physics, University of California, 1156 High Street, Santa Cruz, CA 95064; joel@scipp.ucsc.edu, patrik@ucolick.org

⁴ Racah Institute of Physics, The Hebrew University, Jerusalem 91904, Israel; dekel@phys.huji.ac.il

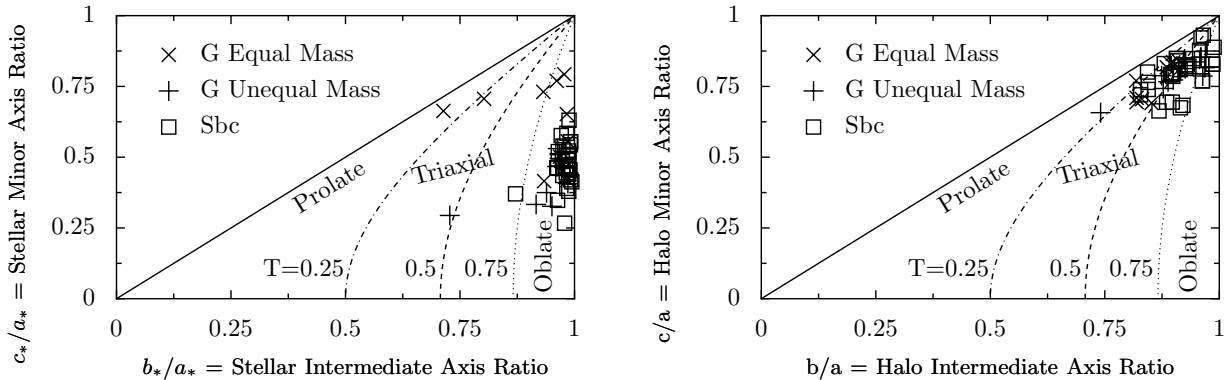


FIG. 1.— Shapes of the luminous and dark components of simulated merger remnants. *Left*: the intermediate-to-major axis ratio vs. the minor-to-major axis ratio for stars. *Right*: Same as left panel, but for dark matter halos. Objects near the diagonal line are prolate spheroids, objects near $b/a = 1$ are oblate spheroids, and objects in between are triaxial. Dotted lines indicate constant triaxiality T . Most stellar remnants are oblate with $\epsilon = 0.5$. Most dark matter halos are either prolate or triaxial.

is enclosed. The result does not appreciably change if equation (1) is modified to include ζ^2 in the denominator. Using a spherical window rather than an ellipsoidal one results in systematically larger axial ratios but does not change the main result.

Three-dimensional shapes of galaxies can be quantified with the triaxiality parameter $T = (a^2 - b^2)/(a^2 - c^2)$. We call an object oblate, triaxial, or prolate if $T < 0.25$, $0.25 < T < 0.75$, or $0.75 < T$, respectively. Shapes of galaxies can also be quantified by ellipticity $\epsilon = 1 - b/a$. Ellipticities are most often used to describe two-dimensional shapes; we occasionally refer to the three-dimensional ellipticity of perfectly prolate or oblate ($T = 0$ or 1) objects since there is no ambiguity about the use of the equation.

Simulations were performed using the entropy-conserving version of the SPH code GADGET (Springel et al. 2001; Springel & Hernquist 2002) with a gravitational smoothing length of 100 pc. The progenitor galaxies have baryonic masses from 1.6×10^9 to $2 \times 10^{11} M_\odot$, gas fractions between 20% and 70%, consist of $\sim 100,000$ particles, and use a parameterization of star formation feedback from supernovae tuned to match the empirical Schmidt law (Kennicutt 1998). Cox (2004) and Cox et al. (2005) contain further information about the simulations.

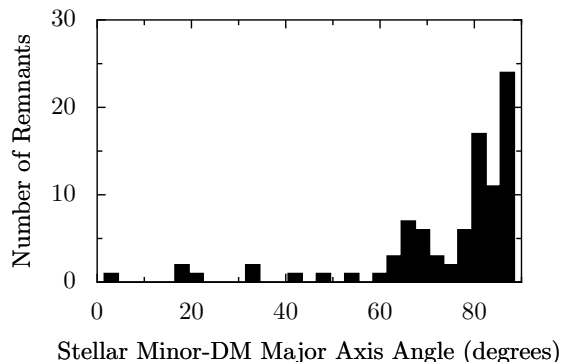


FIG. 2.— The angle between the *minor* axis of the stars and the *major* axis of the dark matter. The stellar material is mostly oblate, the dark matter halos are mostly prolate, and the “preferred” axes of the two shapes are nearly always perpendicular.

3. RESULTS

Figure 1 illustrates that most stellar remnants are oblate, while the dark matter halos in which they reside are mostly prolate or triaxial. Figure 2 shows that the short axis of the stellar system and the long axis of the dark matter halo are almost always nearly perpendicular. This can be understood simply in terms of angular momentum and dissipation, as shown in Figure 3.

This model helps interpret the findings from studies of weak gravitational lensing. Hoekstra et al. (2004) find that the ellipticity of dark halos is $0.77^{+0.18}_{-0.21}$ times the ellipticity of the light (i.e., halos are somewhat less flattened than galaxies), assuming that the two are aligned. According to our result, elliptical galaxies would either show an elliptical halo (if the long axis of the prolate halo is in the plane of the sky) or a circular halo (if the long axis of the halo is pointed toward the observer). Thus, the flattening of the dark matter would follow that of the luminous matter, in agreement with these observations.

The interpretation of the Hoekstra et al. data is com-

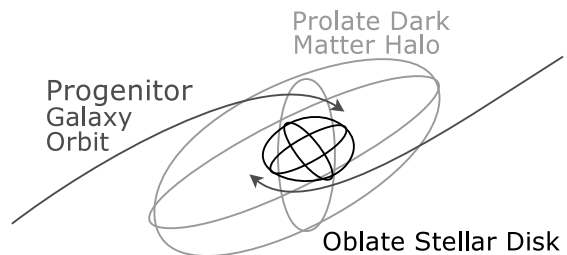


FIG. 3.— The physical interpretation of Figs. 1 and 2 in terms of angular momentum and dissipation. The total angular momentum in a merger simulation is usually dominated by the orbital angular momentum of the two galaxies. As the galaxies merge, both the luminous and dark components acquire angular momentum from the orbits of the progenitors. Their velocity dispersion increases along the axis parallel to the direction of approach, leading to an anisotropic velocity dispersion tensor. Gas in the simulation cools while largely conserving angular momentum so that it spins up to the point where the shape of the resulting stellar system is determined by rotation, not velocity dispersion anisotropy. Meanwhile, the dark matter cannot cool, so its shape is determined by velocity dispersion anisotropy. Therefore, the stellar system is oblate, dark matter halos are prolate, and the angle between the “preferred” axes of these two shapes is $\simeq 90^\circ$.

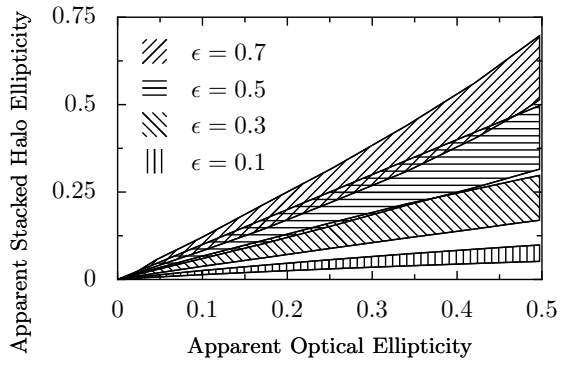


FIG. 4.— Consequences of our model for weak gravitational lensing measurements where one must stack many optically aligned galaxies in order to detect flattening of the dark matter halo. The plot shows the apparent ellipticity of the halo mass surface density vs. the apparent optical ellipticity of the stacked galaxies. Each shaded region shows the range of possible apparent ellipticities given an *intrinsic, three-dimensional* halo ellipticity. The lower bound of each shaded region is given by assuming a prolate halo and the upper bound by assuming an oblate halo. This is the result one would obtain if all galaxies followed the trend noted in this Letter and one stacked galaxies only with a *given* optical ellipticity. The observed halo ellipticity goes to zero for apparent optical ellipticities near zero because the galaxies cannot be oriented so that the stacking is coherent, even though each individual halo will have a nonzero projected ellipticity. The observed halo ellipticity only equals the three-dimensional ellipticity when halos are intrinsically oblate and the galaxies are viewed edge on; otherwise the flattening is underestimated.

plicated by the inclusion of spiral as well as elliptical galaxies in the sample. Mandelbaum et al. (2006a,b) have done a similar study using SDSS galaxies separated by Hubble type and found that the projected halo shapes for elliptical galaxies are aligned with the projected stellar shapes, in agreement with Hoekstra et al. Finally, the projected positions of satellite galaxies also seem to indicate that the projected shapes of elliptical galaxies and halos are aligned (Sales & Lambas 2004; Brainerd 2005; Yang et al. 2006).

Weak lensing studies necessarily underestimate the flattening of dark matter halos. Figures 4 and 5 quantify this by simulating the weak gravitational lensing observations. Given assumptions about the three-dimensional shapes and mass profiles of galaxies and their halos and a scheme for combining many galaxies into a single mass surface density, these two figures show shapes of the projected halo mass surface densities. They allow observers to translate their two-dimensional measurements to a range of possibilities for the three-dimensional structure of dark matter halos.

The hydrodynamic simulations discussed here do not represent a cosmologically unbiased sample, so they are *not* used as input to the simulated lensing observations. Instead we adopt a slightly idealized version of the correlation between halos and galaxies noted in this Letter. Nearly all of the baryonic components of the simulated galaxies are close to 2:1 oblate spheroids, so we assume that all early-type galaxies are so described. Thus, there is a simple mapping between viewing angle and optical ellipticity. We assume all galaxies follow the correlation between halos and galaxies noted here and that the halo mass density is given by a triaxial Navarro-Frenk-White profile: $\rho = \rho_0 / (\zeta / r_s) (1 + \zeta / r_s)^2$, where ρ is the

mass density and ρ_0 is a constant (Navarro et al. 1996; Jing & Suto 2002).

Contopoulos (1956) showed that for a triaxial ellipsoid with constant three-dimensional axis ratios, the contours of constant projected surface density are ellipses with constant ellipticity and position angle, independent of the radial density profile. We only use the ellipticity and position angle of the baryonic component, so the radial profile of the baryons does not matter. The Contopoulos (1956) analysis does not apply to the stacked dark matter halos, so Figures 4 and 5 depend on the radial density distribution of the halos. In practice the difference is not large.

To simulate weak lensing measurements, we align the projected mass distributions based on projected light distributions, stack the projected halo mass distributions, and fit an ellipse to the halo mass surface density distribution where the area of the ellipse is constrained to equal $\pi(3r_s)^2$. This size for the ellipse is motivated by the approximate radius at which weak lensing observations are sensitive to the halo shape (M. J. Hudson 2006, personal communication). The stacking either assumes a given inclination of the optical galaxy, averaging over the azimuthal angle (as in Fig. 4), or assumes that some *minimum* optical ellipticity is required to be included in the stack, averaging over the portion of the unit sphere that gives rise to sufficient optical ellipticities (as in Fig. 5).

Figure 4 shows that galaxies with low optical ellipticities will have low halo ellipticities because there is no preferred axis to use to stack galaxies. The only situation where the projected halo ellipticity equals the three-dimensional halo ellipticity is when all stacked galaxies are viewed edge-on and halos are intrinsically oblate. Flattening is underestimated in all other cases.

Figure 5 shows the result of the more realistic scenario where all galaxies with optical ellipticities greater than some value are included in the stack. This allows one to transform projected ellipticities to three-dimensional ellipticities. For example, if an observer sets the minimum optical ellipticity to 0.2 and measures a stacked halo ellipticity of 0.25, one can conclude that the three-dimensional ellipticity of halos is either 0.3 (for oblate halos), 0.5 (for prolate halos), or somewhere in between.

As one enforces tighter constraints on the optical ellipticity, the halo ellipticity goes up, but the cost is that fewer galaxies will make it into the stack. Under simple assumptions, one can estimate the signal-to-noise ratio (S/N) of the halo ellipticity measurement to be

$$(S/N)_{\text{tot}} = \epsilon_{2D} \sqrt{\Omega N_{\text{tot}}} / \sigma_1 \quad (3)$$

where ϵ_{2D} is the apparent ellipticity of the stacked halo mass surface density, Ω is the solid angle of viewing angles for which a galaxy will be included in the stack, N_{tot} is the total number of galaxies in the survey, and σ_1 is the error on the halo ellipticity when only *one* galaxy is used. We define Ψ as the part of this expression which depends on the signal and the available solid angle:

$$\Psi = \epsilon_{2D} \sqrt{\Omega} \quad (4)$$

Figure 5 thus also allows observers to estimate the quality of their measurement given the size of their survey and an estimate of the one-galaxy error on the halo ellipticity. In reality, observers do not know Ω , but they could estimate

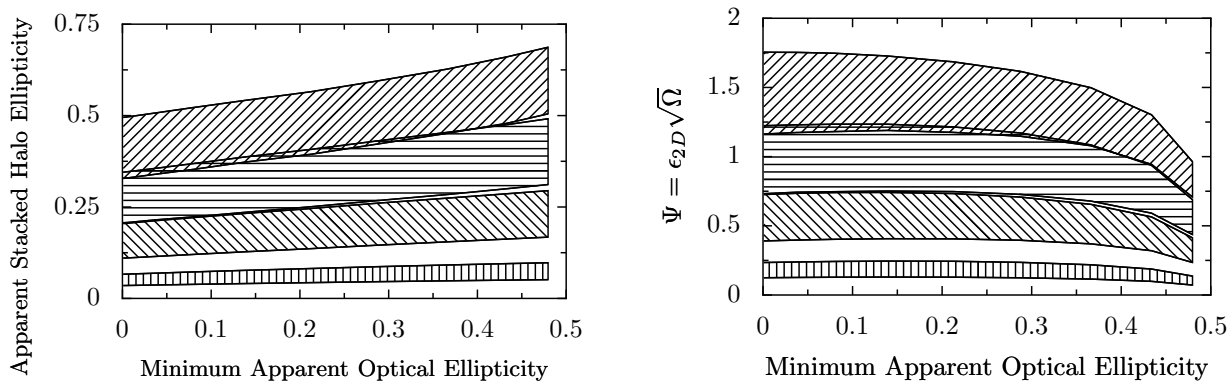


FIG. 5.— Weak gravitational lensing measurements when all galaxies with optical ellipticities greater than some value are included in the stacking. The shaded regions are defined as in Fig. 4. In both panels the x -axis is the minimum apparent optical ellipticity of galaxies included in the stacking. *Left*: The y -axis shows the apparent ellipticity of the stacked halo mass surface density. This is the halo ellipticity that would be measured if one stacked *all* galaxies with optical ellipticity greater than the given value. *Right*: Effect of different optical ellipticity requirements on the S/N ratio of the halo ellipticity measurement. Increasing the minimum optical ellipticity increases the signal (as seen in the right panel) but also increases the noise by reducing the number of galaxies included in the stack. The y -axis is Ψ defined by eq. (4). For small optical ellipticity cuts, the increase in signal is almost exactly canceled by the decrease in available solid angle, meaning that nothing is lost (or gained) by removing round galaxies from the stack. In reality, there is an advantage to removing low-ellipticity galaxies since their position angle is ill-defined. (This analysis assumes no error in position angle.) Above a minimum ellipticity of ~ 0.25 the quality of the measurement declines rapidly because of smaller solid angle of available viewing directions.

it from the from the minimum ellipticity of galaxies in their sample as long as our assumption that the stellar remnants are 2:1 oblate spheroids is not far wrong.

4. DISCUSSION

We have analyzed the three-dimensional shapes of galaxies and dark matter halos resulting from more than 100 simulations of gas-rich galaxy mergers. Stellar remnants are nearly all oblate, with a few examples of triaxiality in the most gas-poor mergers. Dark matter halos are either prolate or triaxial, and the short axis of the baryons is perpendicular to the long axis of the dark matter. All of these facts can be understood in terms of the effects of angular momentum and dissipation during the merger. If there is a class of elliptical galaxies that were formed by gas-rich binary galaxy mergers, they can be expected to display these characteristics.

Real galaxies in a Λ CDM universe are thought to have experienced many mergers over the course of their history, and these multiple mergers can be expected to weaken the relationship between the shapes of galaxies and their halos described here. The extent to which the effects of large-scale structure, such as mass accretion along filaments, tend to preserve the relationship between galaxies and their halos is an interesting and open question.

G. S. N. was supported by the Krell Institute through the Computational Science Graduate Fellowship Program. Computing resources were provided by the UCSC Beowulf cluster UpsAnd and NERSC. We thank Andreas Burkert, S. M. Faber, Mike Hudson, and Laura Parker for useful discussions.

REFERENCES

- Alam, S. M. K. & Ryden, B. S. 2002, *ApJ*, 570, 610
 Allgood, B., Flores, R. A., Primack, J. R., Kravtsov, A. V., Wechsler, R. H., Faltenbacher, A., & Bullock, J. S. 2006, *MNRAS*, 367, 1781
 Bender, R., Burstein, D., & Faber, S. M. 1992, *ApJ*, 399, 462
 Bender, R., Doebereiner, S., & Moellenhoff, C. 1988, *A&AS*, 74, 385
 Brainerd, T. G. 2005, *ApJ*, 628, L101
 Contopoulos, G. 1956, *Zeitschrift fur Astrophysik*, 39, 126
 Cox, T. J. 2004, PhD thesis, University of California, Santa Cruz
 Cox, T. J., Jonsson, P., Primack, J. R., & Somerville, R. S. 2005, *MNRAS*, submitted, (astro-ph/0503201)
 Dubinski, J. & Carlberg, R. G. 1991, *ApJ*, 378, 496
 Franx, M., Illingworth, G., & de Zeeuw, T. 1991, *ApJ*, 383, 112
 Hoekstra, H., Yee, H. K. C., & Gladders, M. D. 2004, *ApJ*, 606, 67
 Jing, Y. P. & Suto, Y. 2002, *ApJ*, 574, 538
 Kennicutt, R. C. 1998, *ApJ*, 498, 541
 Mandelbaum, R., Hirata, C. M., Ishak, M., Seljak, U., & Brinkmann, J. 2006a, *MNRAS*, 367, 611
 Mandelbaum, R., Seljak, U., Kauffmann, G., Hirata, C. M., & Brinkmann, J. 2006b, *MNRAS*, 368, 715
 Naab, T. & Burkert, A. 2003, *ApJ*, 597, 893
 Navarro, J. F., Frenk, C. S., & White, S. D. M. 1996, *ApJ*, 462, 563
 Robertson, B., Cox, T. J., Hernquist, L., Franx, M., Hopkins, P. F., Martini, P., & Springel, V. 2006, *ApJ*, 641, 21
 Sales, L. & Lambas, D. G. 2004, *MNRAS*, 348, 1236
 Springel, V. & Hernquist, L. 2002, *MNRAS*, 333, 649
 Springel, V., Yoshida, N., & White, S. D. M. 2001, *New Astronomy*, 6, 79
 Vincent, R. A. & Ryden, B. S. 2005, *ApJ*, 623, 137
 Yang, X., van den Bosch, F. C., Mo, H. J., Mao, S., Kang, X., Weinmann, S. M., Guo, Y., & Jing, Y. P. 2006, *MNRAS*, 369, 1293